Multipoint Raman Spectrometer Based on a Time-Resolved CMOS SPAD Sensor

Tuomo Talala, Ville A. Kaikkonen, Eetu Virta, Anssi J. Mäkynen, and Ilkka Nissinen, *Member, IEEE*

***Abstract*— The potential of in-line Raman spectrometers for process monitoring applications has been shown for many industrial processes, but in most cases, only one measurement point has been monitored by one spectrometer. In this letter, we describe and demonstrate a novel, time-resolved method for measuring Raman spectra and fluorescence lifetimes from multiple points using a single excitation source and a single spectrometer. This technique is based on a combination of a time-resolved CMOS SPAD (single-photon avalanche diode) line sensor and a fitting optical light guiding system. The line sensor is designed to make multiple individual measurements at intervals of tens of nanoseconds and the optical light guiding system, in turn, produces matching temporal differences for optical signals from different measurement points. Thereby, signals from different points are distinguished in the time domain. A combined Raman and fluorescence lifetime monitoring of two measurement points was demonstrated with an oil-ethanol emulsion sample.**

***Index Terms*— Fluorescence lifetime, Raman spectroscopy, single-photon avalanche diode (SPAD) time-correlated single photon counting (TCSPC), time-resolved spectroscopy.**

I. Introduction

RAMAN spectroscopy has been used for a wide variety of process monitoring applications. For example, blending and crystallization in pharmaceutical processes [1], [2], cell culture bioreactors [3], yeast fermentation [4], food quality [5], and content of polymer blends [6] have been monitored by means of in-line Raman spectroscopy. Typically, only a single point in a process is monitored by one spectrometer, but multipoint measurement setups have also been reported. Gas detection from two measurement points was shown in [7], and a waste water measurement from ten points was demonstrated in [8]. In these systems, the capability for measuring Raman spectra from multiple points is based on the two dimensions of a 2D pixel array of a CCD sensor. While one dimension is used for separating different wavelength Raman scattered photons, the other dimension separates the spectra from different measurement points. This method has also been used for imaging Raman spectroscopy. Raman images of living cells were created by measuring spectra simultaneously from 48 measurement points in [9] and peripheral nerve imaging was made with 32 measurement points in [10]. In both cases, Raman signal from multiple measurement points was collected into a rectangle-to-linear optical fiber bundle that spreads the signals from the different image points as non-overlapping spectra on a CCD sensor. This method is illustrated for two measurement points in Fig. 1 a). Splitting the excitation power to multiple measurement points is especially useful for sensitive samples which cannot withstand the full laser power at a single point (biological samples, for example). Instead of attenuating the excitation, full excitation power can be utilized if it is shared among several measurement points.

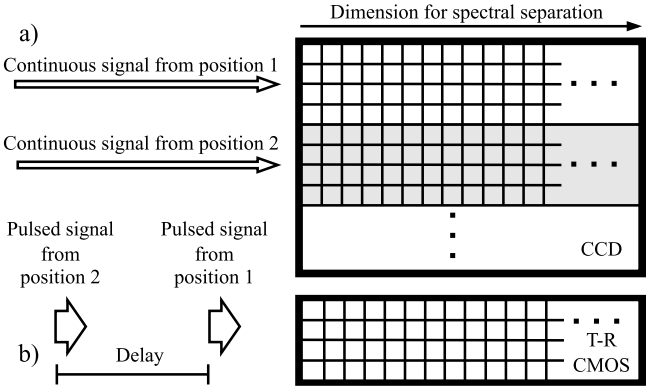

Fig. 1. Multipoint Raman measurement with a) a 2-D CCD sensor, b) a time-resolved CMOS SPAD line sensor.

During the past decade, in addition to the conventional combination of a continuous wave excitation and a CCD sensor, pulsed excitation and time-resolved CMOS SPAD (single photon avalanche diode) line sensors have been used in Raman spectroscopy. The advantages of time-resolved measurements are the abilities to separate the Raman signal from fluorescence emission in the time domain [11], to measure the fluorescence lifetime to give additional information about the sample [12], and to make depth-resolved measurements [13].

In this work, we describe and demonstrate a novel method for measuring Raman spectra from multiple points using a single excitation source and a single time-resolved spectrometer. This method is based on two essential components. The first component, a time-resolved CMOS SPAD line sensor, is designed to be able to make multiple measurements at intervals of some tens of nanoseconds. The second component, an optical fiber and probe system for excitation and Raman signal collection, generates a matching arrival time difference for the signals from the different measurement points. As a result, Raman signals from multiple measurement points are separated in the time domain, and the whole active area of the 2D sensor can be utilized for all measurement points as

Manuscript received 3 November 2022; revised 3 April 2023; accepted 16 April 2023. Date of publication 19 April 2023; date of current version 28 April 2023. This work was supported by the Academy of Finland under Contract 314404, Contract 314405, and Contract 323719. *(Corresponding author: Tuomo Talala.)*

Tuomo Talala, Eetu Virta, and Ilkka Nissinen are with the Circuits and Systems Research Unit, University of Oulu, 90014 Oulu, Finland (e-mail: tuomo.talala@oulu.fi).

Ville A. Kaikkonen and Anssi J. Mäkynen are with the Optoelectronics and Measurement Techniques Research Unit, University of Oulu, 90014 Oulu, Finland.

Color versions of one or more figures in this letter are available at https://doi.org/10.1109/LPT.2023.3268333.

Digital Object Identifier 10.1109/LPT.2023.3268333

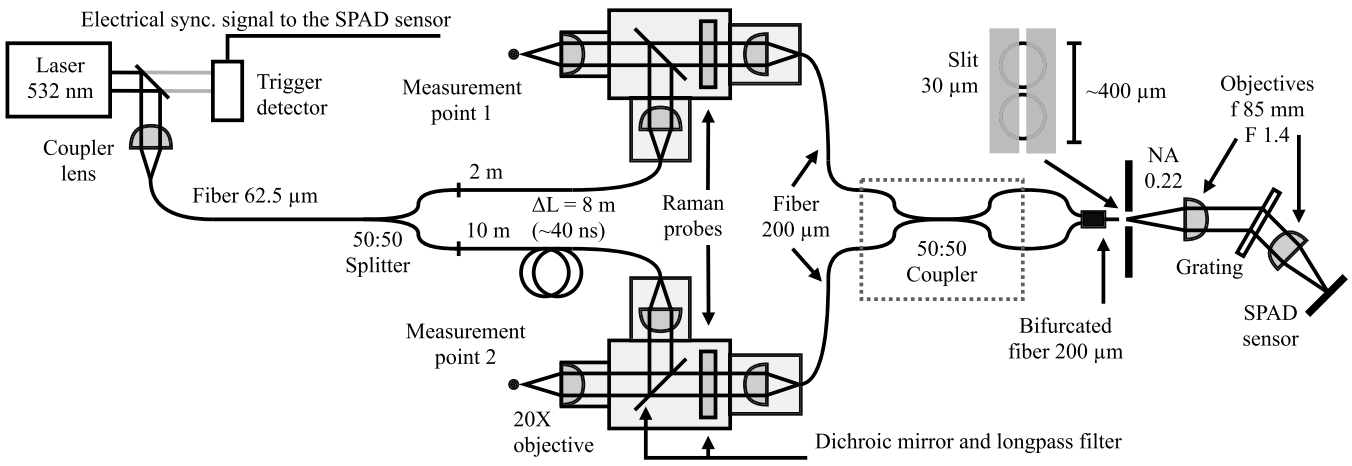

Fig. 2. Multipoint Raman spectrometer setup.

illustrated in Fig. 1 b). Naturally, all the other previously mentioned advantages of the time-resolved measurement are available for the multipoint measurement too.

II. Design

An optical light guiding system for a single excitation source and a single line sensor setup utilizing multiple temporally separated measurement points has three main specifications. Firstly, it should split the excitation laser pulse spatially to different measurement points. Secondly, it should combine the collected Raman photons from the different measurement points on the same optical path. Lastly, it should generate a constant temporal delay to the Raman photons from the different measurement points. An all-fiber optical split and combination system without moving parts was chosen as the light guiding method to reach these specifications. This also makes the system robust and easily adaptable for different distances and numbers of the measurement points. The designed multipoint spectrometer shown in Fig. 2 consists of a pulsed laser source (Teem Photonics ANG-150P-000, 532 nm, 140 kHz, 150 ps FWHM, 68 mW average power), light guiding fiber optics and couplers, two fiber-optic Raman probes, a unity magnification spectrometer, and a time-resolved CMOS SPAD line sensor.

A prototype for two measurement points was constructed and tested in laboratory environment. It consists of of-the-shelf multimode (MM) fiber optical patch cables and components together with two Raman probes (Thunder Optics S.A.S., minimum 175 cm^{-1} Raman shift model) which have SMA fiber connectivity and 20x objective lenses. Graded index optical fiber cables were used in the excitation pulse guiding to minimize modal dispersion, but the downside compared with step index fibers is a higher attenuation of the pulse energy.

A small fraction of the excitation laser is first split to the trigger detector (Thorlabs DET025A/M) and the other part is coupled (Thorlabs CFC-11X-A) into a 62.5 micron graded-index fiber (Thorlabs GIF625), which is then butt coupled into a 50:50 ratio fused fiber optic splitter (TG625R5F1). The two outputs of the fiber splitter are then butt-coupled to two patch fibers of different lengths (2 m and 10 m) which are connected to the Raman probes, resulting in a temporal difference on the arrival of the excitation pulses on the probes. The 8 m difference in the excitation fiber lengths corresponds roughly a timing difference of 40 ns, which matches the interval between the consecutive measurements on the SPAD sensor.

The collected Raman signals from the probes are coupled to 200 micron core diameter equal length MM fibers (Thorlabs M36L01). These fibers from the probes are butt-coupled into a 2 × 2 fused fiber optical 50:50 ratio coupler (Thorlabs TM200R5F2B). The combiner couples half of the Raman signal from both probes to the two output fibers, which are then butt-coupled into a bifurcated fiber patch cable (Avantes FCB-UVIR200-2). The bifurcated cable features two adjacent fiber ends in a single connector, which is placed directly behind the slit of the spectrometer so that the fiber ends are in line with the slit.

Part of the light from the fiber ends passes through the 30 μm wide slit (Thorlabs S30K) and is then collimated using an 85 mm focal length camera objective (Samyang Optics, 85mm f/1.4 AS IF UMC). The collimated light is dispersed using a transmission grating with 1800 lines/mm (Wasatch Photonics). Next, the dispersed light from the grating is focused on the SPAD sensor using an identical camera objective as for the collimation.

The sensor of the spectrometer, a SPAD line sensor manufactured in 110-nm CMOS technology, is designed for time-correlated single photon counting (TCSPC) applications, especially for time-resolved Raman spectroscopy. The main parts of the sensor are a 256 × 8 SPAD array and 256 time-to-digital converters (TDCs). Temporal resolution of the 7-bit TDCs can be adjusted over a range of 25.6–65 ps, and the pitch and the fill-factor of the SPAD array are 32.9 μm and 37.9%, respectively. Data read-out and controlling of sensor operation are done with an Opal Kelly XEM7310-A200 FPGA integration module. A detailed description for the sensor is given in [14].

A key feature for multipoint Raman measurements is the triple measurement operation mode of the sensor. In the triple measurement mode, the sensor repeats a normal measurement three times at intervals of tens of nanoseconds for each excitation pulse (the exact interval between three measurements can be adjusted in a range of ∼35–100 ns). SPADs

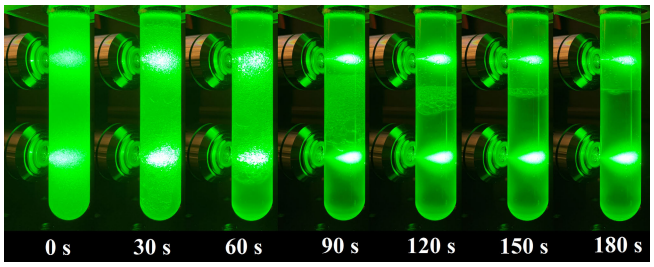

Fig. 3. Photographs of a sunflower oil-ethanol emulsion.

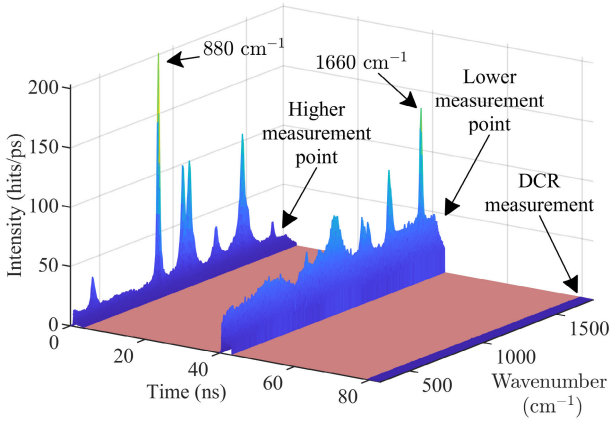

Fig. 4. Mean triple measurement data of sunflower oil-ethanol emulsion monitoring for a period of 160–180 s.

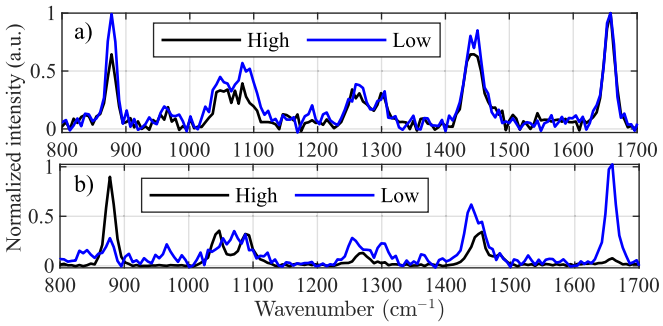

Fig. 5. Normalized spectra of sunflower oil-ethanol emulsion at a) 0–2 s, and b) 178–180 s.

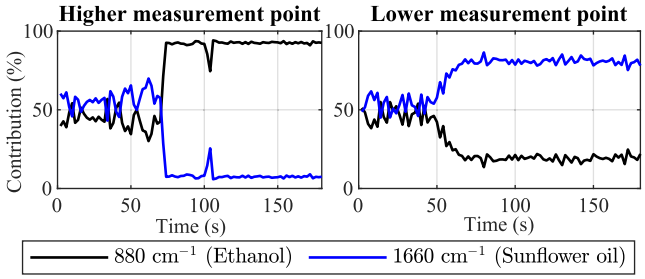

Fig. 6. Contributions of Raman signals at 880 cm^{-1} and 1660 cm^{-1} to the total Raman signal during the 180 s period.

are loaded separately for these three measurements and they are actively quenched between the measurements. Therefore, measurements are completely separate, i.e. photon detections during previous measurements do not affect the subsequent measurements. The three TCSPC measurement results from each excitation pulse are initially stored to the registers on the sensor chip and then transferred to the FPGA which accumulates 768 (3 · 256) TCSPC histograms.

III. Results

To demonstrate the multipoint Raman measurement, an oil-ethanol emulsion was measured. The interest in such a sample is related to its potential as an alternative fuel for diesel engines [15], [16]. An emulsion of pure ethanol (Etax Aa) and edible sunflower oil was made into a test tube, and the composition of the mixture was monitored for a 180-second observation period (90 measurements, 2 s each) at two measurement points at different heights as shown in Fig. 3. The measured average power directly from the laser was 68 mW, and from each Raman probe the power was measured to be 18 mW.

The first measurement of the triple measurement mode collects a signal from the higher measurement point and the second measurement collects a signal from the lower measurement point. The third measurement is made without excitation and can therefore be used as a real-time dark count rate (DCR) measurement. An averaged result of the last ten measurements (the last 20 s) is shown in Fig. 4. In Fig. 4, three blue sections are the three measurements of the triple measurement mode. The spectrum of ethanol dominates at the higher measurement point and the spectrum of sunflower oil at the lower measurement point. During the red sections between the measurements, SPADs are quenched and the sensor is not detecting photons.

Normalized Raman spectra from the higher (black line) and the lower (blue line) measurement points are shown in Fig. 5 a) for the first two-second acquisition time. These two spectra are quite similar which is expected as the emulsion is fairly homogeneous right after mixing. Normalized Raman spectra for the last two-second acquisition are shown in Fig. 5 b). The Raman peak of ethanol at 880 cm^{-1} and the Raman peak of sunflower oil at 1660 cm^{-1}clearly show that the components of the emulsion have separated; oil is on the bottom and ethanol is on the top. Compared with spectra in Fig. 5 b), the SNR of spectra in Fig. 5 a) is lower due to low signal level caused by the opacity of the emulsion. Time gate width of 810 ps (TDC bins 11–40, resolution 27 ps) was used for spectra in Fig. 5. Post-processing steps for spectra in Fig. 5 are dark count subtraction and baseline subtraction (DCR measured by the third measurement of the triple measurement mode, baseline estimated by the asymmetric least squares smoothing [17]).

A percentage contributions of Raman signals at 880 cm^{-1} and at 1660 cm^{-1} to the total Raman signal are shown as a function of time in Fig. 6 (the sum of Raman signals at 880 cm^{-1} and 1660 cm^{-1} was used as a total Raman signal, the other wavenumbers were ignored). Even with this extremely simple data processing, the separation of contents is clearly shown in Fig. 6. Curves in Fig. 6 agree well with Fig. 3, where the photographs show that at 60 s, the emulsion has not yet separated at measurement points but at 90 s, the contents appear transparent at both measurement points and emulsion only exists in the middle of the test tube.

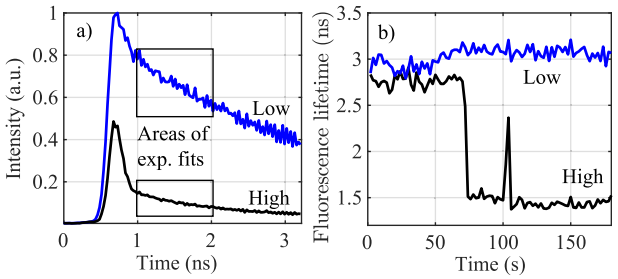

Fig. 7. a) TCSPC histogram at 178–180 s (average of 256 channels). b) Fluorescence lifetimes during the 180 s period.

TCSPC histograms (average of all 256 channels) of both measurement points for a period of 178–180 s are shown in Fig. 7 a). The histogram of the higher measurement point consists of a clear pulsed part at 0.5–1 ns (Raman signal from the ethanol) and a weak tail after 1 ns (the combination of fluorescence emission from oil residues and a diffusion tail of the pulsed Raman signal). The histogram of the lower measurement part is dominated by fluorescence emission from the oil but also a pulsed part at 0.5–1 ns can be observed.

Fluorescence lifetimes were estimated from TCSPC histograms by fitting a single-term exponential fit to a part of the fluorescence tail at 1–2 ns and the results are shown in Fig. 7 b). At lower measurement point, the fluorescence lifetime is approximately constant ∼3 ns for the whole 180 s period. This indicates that sunflower oil exists at lower part of the test tube for the whole observation period. At the higher measurement point, the fluorescence lifetime stays at ∼2.8 ns for a period of 72 s and then quickly decreases to ∼1.5 ns clearly showing that the top surface of the emulsion drops below the higher measurement point. After that, mainly ethanol is measured at the higher measurement point. The only clear exception is an occasional oil drop that is observed at 102–104 s. This oil drop can be noticed by Raman monitoring (Fig. 6 a)) and by fluorescence lifetime monitoring (Fig. 7 b)) alike. It should be noted that the absolute accuracy of these fluorescence lifetime estimates is low because the instrument response function (IRF) of the system was not characterized and compensated for. However, the relative changes of the fluorescence lifetime can be seen clearly even without any compensation for the IRF.

IV. Conclusion

A novel method for multipoint Raman measurements using a single excitation source and a single spectrometer was described and demonstrated. In this technique, a time-resolved CMOS SPAD line sensor together with an optical fiber setup are utilized to distinguish optical signals from different measurement points in the time domain. The demonstrative oil-ethanol emulsion measurement proved that this technique can be used to monitor multiple measurement points with combined Raman and fluorescence lifetime measurements. Though this prototype was built for two measurement points, for potential applications such as industrial process monitoring, both the sensor and the fiber-optic system can be modified for higher number of measurement points. Additionally, the optical performance can be improved by replacing off-the-shelf components with custom-made parts to have fewer fiber joints and hence a reduced signal attenuation in the optical path.

References

[1] G. J. Vergote et al., "In-line monitoring of a pharmaceutical blending process using FT-Raman spectroscopy," *Eur. J. Pharmaceutical Sci.*, vol. 21, no. 4, pp. 479–485, Mar. 2004, doi: 10.1016/j.ejps.2003.11.005.

[2] G. Févotte, "In situ Raman spectroscopy for in-line control of pharmaceutical crystallization and solids elaboration processes: A review," *Chem. Eng. Res. Design*, vol. 85, no. 7, pp. 906–920, 2007, doi: 10.1205/cherd06229.

[3] N. R. Abu-Absi et al., "Real time monitoring of multiple parameters in mammalian cell culture bioreactors using an in-line Raman spectroscopy probe," *Biotechnol. Bioeng.*, vol. 108, no. 5, pp. 1215–1221, 2011, doi: 10.1002/bit.23023.

[4] R. Schalk et al., "Non-contact Raman spectroscopy for in-line monitoring of glucose and ethanol during yeast fermentations," *Bioprocess Biosyst. Eng.*, vol. 40, no. 10, pp. 1519–1527, Oct. 2017, doi: 10.1007/s00449-017-1808-9.

[5] T. A. Lintvedt, P. V. Andersen, N. K. Afseth, B. Marquardt, L. Gidskehaug, and J. P. Wold, "Feasibility of in-line Raman spectroscopy for quality assessment in food industry: How fast can we go?" *Appl. Spectrosc.*, vol. 76, no. 5, pp. 559–568, May 2022, doi: 10.1177/00037028211056931.

[6] S. Zhu, Z. Song, S. Shi, M. Wang, and G. Jin, "Fusion of near-infrared and Raman spectroscopy for in-line measurement of component content of molten polymer blends," *Sensors*, vol. 19, no. 16, p. 3463, Aug. 2019, doi: 10.3390/s19163463.

[7] C. Shen, C. Wen, X. Huang, and X. Long, "A versatile multiple-pass Raman system for industrial trace gas detection," *Sensors*, vol. 21, no. 21, p. 7173, Oct. 2021, doi: 10.3390/s21217173.

[8] T. M. Vess and S. M. Angel, "Near-visible Raman instrumentation for remote multipoint process monitoring using optical fibers and optical multiplexing," in *Environ. Process Monitor. Technol.*, vol. 1637, pp. 118–125, 1992, doi: 10.1117/12.59330.

[9] M. Okuno and H.-O. Hamaguchi, "Multifocus confocal Raman microspectroscopy for fast multimode vibrational imaging of living cells," *Opt. Lett.*, vol. 35, no. 24, p. 4096, Dec. 2010, doi: 10.1364/ol.35.004096.

[10] Y. Kumamoto, Y. Harada, H. Tanaka, and T. Takamatsu, "Rapid and accurate peripheral nerve imaging by multipoint Raman spectroscopy," *Sci. Rep.*, vol. 7, no. 1, p. 845, 2017, doi: 10.1038/s41598-017-00995-y.

[11] J. Kostamovaara, J. Tenhunen, M. Kögler, I. Nissinen, J. Nissinen, and P. Keränen, "Fluorescence suppression in Raman spectroscopy using a time-gated CMOS SPAD," *Opt. Exp.*, vol. 21, no. 25, p. 31632, Dec. 2013, doi: 10.1364/oe.21.031632.

[12] G. Giraud et al., "Fluorescence lifetime biosensing with DNA microarrays and a CMOS-SPAD imager," *Biomed. Opt. Exp.*, vol. 1, no. 5, p. 1302, Dec. 2010, doi: 10.1364/boe.1.001302.

[13] J. Kekkonen, J. Nissinen, and I. Nissinen, "Depth analysis of semi-transparent media by a time-correlated CMOS SPAD line sensor-based depth-resolving Raman spectrometer," *IEEE Sensors J.*, vol. 19, no. 16, pp. 6711–6720, Aug. 2019, doi: 10.1109/JSEN.2019.2913222.

[14] T. Talala, E. Parkkinen, and I. Nissinen, "CMOS SPAD line sensor with fine-tunable parallel connected time-to-digital converters for Raman spectroscopy," *IEEE J. Solid-State Circuits*, pp. 1–12, 2022, doi: 10.1109/JSSC.2022.3212549.

[15] M. S. Kumar, J. Bellettre, and M. Tazerout, "The use of biofuel emulsions as fuel for diesel engines: A review," *Proc. Inst. Mech. Eng., A, J. Power Energy*, vol. 223, no. 7, pp. 729–742, Nov. 2009, doi: 10.1243/09576509JPE758.

[16] N. Arpornpong, C. Attaphong, A. Charoensaeng, D. A. Sabatini, and S. Khaodhiar, "Ethanol-in-palm oil/diesel microemulsion-based biofuel: Phase behavior, viscosity, and droplet size," *Fuel*, vol. 132, pp. 101–106, Sep. 2014, doi: 10.1016/j.fuel.2014.04.068.

[17] P. H. Eilers and H. F. Boelens, "Baseline correction with asymmetric least squares smoothing," Leiden Univ. Med. Centre Rep., Leiden, The Netherlands, Oct. 2005, p. 5, vol. 1, no. 1.